Temporal coherency between receptor expression, neural activity and AP-1-dependent transcription regulates *Drosophila* motoneuron dendrite development

Fernando Vonhoff[1,4,*], Claudia Kuehn[1], Sonja Blumenstock[1], Subhabrata Sanyal[2] and Carsten Duch[1,3]

SUMMARY

Neural activity has profound effects on the development of dendritic structure. Mechanisms that link neural activity to nuclear gene expression include activity-regulated factors, such as CREB, Crest or Mef2, as well as activity-regulated immediate-early genes, such as *fos* and *jun*. This study investigates the role of the transcriptional regulator AP-1, a Fos-Jun heterodimer, in activity-dependent dendritic structure development. We combine genetic manipulation, imaging and quantitative dendritic architecture analysis in a *Drosophila* single neuron model, the individually identified motoneuron MN5. First, Dα7 nicotinic acetylcholine receptors (nAChRs) and AP-1 are required for normal MN5 dendritic growth. Second, AP-1 functions downstream of activity during MN5 dendritic growth. Third, using a newly engineered AP-1 reporter we demonstrate that AP-1 transcriptional activity is downstream of Dα7 nAChRs and Calcium/calmodulin-dependent protein kinase II (CaMKII) signaling. Fourth, AP-1 can have opposite effects on dendritic development, depending on the timing of activation. Enhancing excitability or AP-1 activity after MN5 cholinergic synapses and primary dendrites have formed causes dendritic branching, whereas premature AP-1 expression or induced activity prior to excitatory synapse formation disrupts dendritic growth. Finally, AP-1 transcriptional activity and dendritic growth are affected by MN5 firing only during development but not in the adult. Our results highlight the importance of timing in the growth and plasticity of neuronal dendrites by defining a developmental period of activity-dependent AP-1 induction that is temporally locked to cholinergic synapse formation and dendritic refinement, thus significantly refining prior models derived from chronic expression studies.

KEY WORDS: Transcription factor, Neural activity, Dendritic growth, Acetylcholine receptors

INTRODUCTION

Dendritic structure provides the blueprint for neuronal connectivity (Cline, 2001; Libersat and Duch, 2004) and information flow through circuits (Koch and Segev, 2000; London and Häusser, 2005). The development of dendritic structure is influenced by multiple intrinsic and external factors, including neural activity (Cline, 2001; West et al., 2002; Chen and Ghosh, 2005; Sanyal and Ramaswami, 2006).

The *Drosophila* genetic model has yielded useful insights into the molecular basis underlying neuron type-specific dendritic morphology (Moore et al., 2002; Jefferis et al., 2001; Komiyama, Luo, 2007), dendritic spacing (Zhu and Luo, 2004; Grueber et al., 2002; Grueber et al., 2003; Corty et al., 2009) and dendritic guidance (Komiyama et al., 2002; Sweeney et al., 2002; Furrer et al., 2003; Mauss et al., 2009; Brierley et al., 2009). By contrast, few studies have addressed the role of neuronal activity during dendritic development in the *Drosophila* CNS (Tripodi et al., 2008; Hartwig et al., 2008; Duch et al., 2008).

Correct dendrite morphology development requires rapid local signals for individual branch extension and retraction as well as slower global signals for overall arbor growth (Bestman et al., 2008). Synaptic activity provides a means for rapid local changes (Lohmann and Wong, 2005; Lohmann et al., 2002; Niell et al.,

2004). However, in vertebrates, both local changes in dendritic calcium concentrations as well as global changes in calcium throughout the neuron can initiate long-term global changes in gene expression via activity-dependent regulators, such as CREB or Crest (West et al., 2002; Flavell and Greenberg, 2008; Redmond, 2008). Similarly, in *Drosophila*, increased firing activity promotes dendritic overgrowth in developing larval (Hartwig et al., 2008) and adult motoneurons (Duch et al., 2008). In larval motoneurons, activity-induced overgrowth requires the transcription factor AP-1 (Hartwig et al., 2008), a heterodimer of Fos and Jun (Curran and Franza, 1988), encoded in *Drosophila* by the genes *kayak* and *Jra* (*Jun-related antigen*), respectively.

The transcription of both components of AP-1, the immediate-early genes *Fos* and *Jun*, occurs rapidly in response to membrane depolarization and calcium influx (Greenberg et al., 1986; Lamph et al., 1988; Saffen et al., 1988), and in vertebrates *Fos* expression is routinely used as marker for neuronal activity (Morgan et al., 1987; Hunt et al., 1987; Mack and Mack, 1992; Guthrie et al., 1993). Similarly, AP-1-dependent transcription is thought to be controlled by activity, but direct evidence for this hypothesis is lacking (Freeman et al., 2010; Kaczmarek and Chaudhuri, 1997).

By combining genetic manipulation, imaging and quantitative dendritic architecture analysis of one identified *Drosophila* motoneuron, the flight motoneuron MN5 (Ikeda and Koenig, 1988), this study shows that (1) AP-1 and excitatory nicotinic acetylcholine receptors (nAChRs) are required for normal dendritic growth of MN5, (2) activity causes increased AP-1 transcriptional activity via Calcium/calmodulin-dependent protein kinase II (CaMKII) activation during a defined period of pupal development, and (3) activity and AP-1 expression in MN5 can either promote or inhibit dendritic branching, depending on the timing of AP-1 activation.

[1]School of Life Sciences, Arizona State University, Tempe, AZ 85287, USA.
[2]Departments of Cell Biology and Neurology, Emory University School of Medicine, Atlanta, GA 30322, USA. [3]Institute of Neurobiology, Johannes-Gutenberg University Mainz, 55099 Mainz, Germany. [4]Department of Molecular, Cellular and Developmental Biology, Yale University, New Haven, CT 06520, USA.

*Author for correspondence (fernando.vonhoff@yale.edu)

MATERIALS AND METHODS

Animals

Drosophila melanogaster were reared as previously described (Vonhoff and Duch, 2010; Vonhoff et al., 2012). Motoneuron GAL4 driver lines were: (1) w; P103.3-GAL4, UAS-mCD8-GFP;+, (2) C380-GAL4, UAS-mCD8-GFP;; Cha-GAL80 and (3) w;UAS-mCD8-GFP; D42-GAL4, Cha-GAL80. All express in a subset of motoneurons including MN5, but also in some non-identified sensory neurons and interneurons (Yeh et al., 1995; Sanyal et al., 2003; Sanyal, 2009; Budnik et al., 1996; Consoulas et al., 2002; Watson et al., 2008). The Cha-GAL80 transgene was included to inhibit expression in non-identified cholinergic sensory neurons and interneurons. UAS-*fos*; UAS-*jun* and UAS-Jbz strains have been described previously (Eresh et al., 1997; Sanyal et al., 2002; Franciscovich et al., 2008). The w;; *kayak*-GAL4, UAS-nls-GFP was used as a reporter for *fos* (Freeman et al., 2010). The UAS-TrpA1 (Pulver et al., 2009) strain was obtained from Dr L. Griffith (Brandeis University, MA, USA). The Dα7nACh-GAL4 strain (Fayyazuddin et al., 2006) was obtained from Dr H. Bellen (Baylor College of Medicine, Houston, TX, USA). The strain w; TubP-GAL80ts, UAS-mCD8-GFP was used for conditional, temperature-controlled suppression of GAL4 (McGuire et al., 2003).

Production of the AP-1 reporter fly strain

A transgenic strain to report AP-1-dependent transcription was developed by first synthesizing both strands of an artificial enhancer oligonucleotide with four consensus AP-1 binding sites each separated by 15-20 nucleotides. The oligonucleotide was designed such that when the two complementary strands were annealed, they would create overhangs that are compatible with *Xho*I (5′) and *Bam*HI (3′) restriction sites. Double-stranded oligonucleotides were reconstituted by mixing complementary strands, heating for 5 minutes at 98°C and then cooling slowly to room temperature followed by placing on ice. A 333-bp region from the *Drosophila elav* promoter that directs weak expression in the fly nervous system was then amplified from the full promoter (generous gift of Kalpana White) (Yao and White, 1994) with primers that contained an *Eco*RI site at the 5′ end and an *Xho*I site at the 3′ end. This amplicon was digested with the two specific restriction enzymes. Next, the pH-Stinger vector (Barolo et al., 2000) was double digested with *Eco*RI and *Bam*HI. Cloning was carried out by ligating the AP-1 binding site oligonucleotide, the 333-bp *elav* enhancer and the digested pH-Stinger. The resultant construct carried the minimal *elav* promoter (this portion was hypothesized to provide neuronal specificity to the AP-1 reporter without driving strong neuronal expression by itself) (Barolo and Posakony, 2002) upstream of the AP-1 binding sites and controlled expression of nuclear GFP in the pH-Stinger vector. Transgenic flies were made by Rainbow Transgenic Flies (Camarillo, CA, USA) using standard embryo microinjection protocols. The AP-1 binding oligonucleotide sequences are as follows (the putative AP-1 binding sites are underlined): Oligo 1: 5′-GATCCAATCAAA-ACTGTCTGAGTCACTCAGGGATTGGCTGAGTATGAGTCAGCCTC-GAAAATCAAAACTGTCTGAGTCACTCAGGGATTGGCTGAGTAT-GAGTCACTC-3′; Oligo 2: 5′-TCGAGAG<u>TGACTCA</u>TACTCAGCCA-ATCCC<u>TGAGTGA</u>CTCAGACAGTTTTGATTTTCGAGGC<u>TGACTCA</u>-TACTCAGCCAATCCC<u>TGAGTGA</u>CTCAGACAGTTTTGATTG-3′.

Intracellular staining and immunohistochemistry

Intracellular dye injections were conducted as previously described (Duch et al., 2008). Fos-GFP and mCD8-eGFP were detected with an anti-GFP antibody (Invitrogen, rabbit anti-GFP, A11122). The Dα7 nAChR antibody (rat anti-Dα7 nAChR) was a kind gift of Dr H. Bellen. AB specificity has previously been demonstrated by absence of immunosignal in null mutants (Fayyazuddin et al., 2006). For Dα7 nAChR immunocytochemistry, tissue was fixed for 30 minutes in 4% paraformaldehyde, washed in PBS (0.1 mM) overnight, and washed for 3 hours in PBS containing 0.5% Triton X-100. Primary rat anti-Dα7 nAChR antibody was applied for 48 hours at 4°C (1:2000 in PBS containing 0.5% Triton X-100 and 3% bovine albumin serum). GFP antibody was applied at a concentration of 1:1000 in PBS containing 0.5% Triton X-100 and 3% bovine albumin serum. Following primary antibody incubation, preparations were washed in PBS buffer (6×30 minutes) and secondary antibodies were incubated for 12 hours at 4°C (Cy2-conjugated goat anti-rabbit or Cy5-conjugated goat anti-rat; both 1:500 in 0.1 mM PBS). Then preparations were washed in PBS buffer (6×30 minutes), dehydrated in an ascending ethanol series (50, 70, 90, 100%; 15 minutes each), and cleared and mounted in methyl salicylate.

Confocal microscopy, geometric reconstructions and quantitative morphometry

Digital images were captured with a Leica TCS SP2 confocal laser scanning microscope (Bensheim, Germany) using a Leica HCX PL APO CS 40×oil-immersion objective (NA: 1.2) as previously described (Boerner and Duch, 2010). Geometric reconstructions were conducted with custom Amira (AMIRA 4.1.1 software, TGS) plug-ins as previously described (Schmitt et al., 2004; Evers et al., 2005). Data were exported to Microsoft Excel and Statistica (StatSoft, Hamburg, Germany) for further analyses. For figure production, images were exported as TIFF files and further assembled and labeled in figure panels with CorelDraw13 (Corel Corporation).

Live-cell imaging and quantification of AP-1 reporter fluorescence in MN5

For live-cell imaging of MN5 nuclear GFP content upon AP-1 reporter activation, animals were dissected along the dorsal midline and perfused with physiological saline at 24°C under a Zeiss Axiscope 2FS plus fixed-stage fluorescence microscope as described in previous studies on MN5 physiology (Ryglewski and Duch, 2009; Ryglewski et al., 2012). MN5 was identified by retrograde labeling with the lipophilic dye DiI (Invitrogen, D3899). DiI was injected into the dorsal-most fibers of the DLM flight muscle 12 hours prior to imaging (Fig. 2A,B). Live images of DiI-labeled MN5 and nuclear AP-1 reporter GFP signals were acquired with a cooled CCD camera (Hamamatsu 4742-95) and simple PCI software (Compix). Image resolution was 1024×1024 pixels. All MN5 nuclei were imaged with identical filter and camera settings (exposure time of 0.02 seconds), saved as TIFF files and exported to ImageJ. MN5 nucleus was defined as the region of interest and GFP fluorescence was measured as the mean gray value within that region. Background fluorescence was routinely subtracted.

RESULTS

AP-1 is transcriptionally active during dendrite growth in MN5

MN5 is a monopolar motoneuron that can be identified unambiguously by its characteristic location and morphology (Coggshall, 1978; Consoulas et al., 2002). It innervates the contralateral, dorsal-most two fibers of the dorsolongitudinal flight muscle (DLM) (Ikeda and Koenig, 1988), which produces the power for wing downstroke during *Drosophila* flight. MN5 has a stereotyped dendritic structure comprising a total length of 6500 μm and >4000 branches (Vonhoff and Duch, 2010). Although MN5 is born during embryonic development, it is developmentally arrested during larval life, and all dendrites develop *de novo* during pupal life (Fig. 1A-C) (Consoulas et al., 2002). The first dendritic branches extend off the primary neurite at early pupal stage P5 [~12.5 hours after puparium formation (APF)] (Fig. 1A, arrowheads). By pupal stage P7 (~40 hours APF) all first order dendrites have formed and higher order branches develop (Fig. 1B). At pupal stage P15 (~90 hours APF, pharate adult), the dendritic tree of MN5 is adult-like (Fig. 1C).

Increased MN5 excitability induced by expression of dominant-negative transgenes for Shaker and Eag potassium channels [using the recombinant chromosome EKI (electrical knock-in)] significantly increases dendritic branching (Duch et al., 2008). Work on larval *Drosophila* motoneurons indicated a role of AP-1 in activity-dependent dendritic growth (Hartwig et al., 2008). Therefore, we tested whether AP-1 dependent transcription was regulated in MN5 by neuronal activity during pupal life. First, we
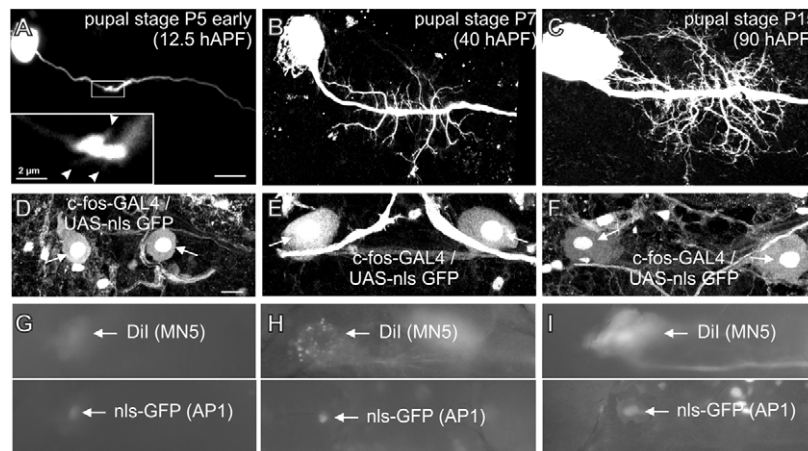
Fig. 1. AP-1 is endogenously expressed and transcriptionally active during all stages of MN5 dendritic growth. (A-C) Representative examples of MN5 dendritic structure at different pupal stages of *Drosophila*. (A) Onset of dendritic outgrowth is evident at pupal stage P5 early [12.5 hours after puparium formation (hAPF)]. Selective enlargement (white box) shows the first three future dendrites emerging from the primary neurite (arrowheads). (B) By pupal stage P7 (~40 hours APF) all major primary dendrites have formed. (C) At pupal stage P15 (~90 hours APF) dendritic structure appears adult-like. Scale bar: 10 μm. **(D-F)** *Fos* reporter (*kayak*-GAL4; UAS-nls-GFP) expression as detected by GFP immunostaining in MN5 nuclei (arrows) during the onset (D; early P5), ongoing (E; P7) and late (F; P15) stages of dendritic growth. Scale bar: 20 μm. **(G-I)** Live images of DiI-labeled MN5 somata (upper row, white arrows) in pupae expressing an AP-1 nls-GFP reporter (lower row, white arrows show nuclear GFP expression) at pupal stages P5 (G), P7 (H) and P15 (I).

verified that *fos* and AP-1 were expressed in MN5 during dendrite development. To test for *fos* expression in MN5 we used a *kayak*-GAL4, UAS-nls-GFP reporter line, in which the expression of GAL4 is regulated by the promoter of the *Drosophila fos* gene, *kayak* (Freeman et al., 2010). Consequently, all cells expressing *fos* endogenously show nuclear GFP localization. Anti-GFP immunocytochemistry in the ventral nerve cord (VNC) revealed *fos* in the nucleus of MN5 through all crucial stages of dendritic growth (Fig. 1D-F, arrow).

We have not directly measured the expression of AP-1 because immunocytochemistry with available antibodies or *in situ* hybridization have not proven reliable in detecting small changes in endogenous Fos and Jun. To specifically monitor transcriptional readout of AP-1 in MN5 we created a new AP-1 reporter line (see Materials and methods), which reports AP-1 induced transcriptional activity by nuclear GFP localization. MN5 was identified by retrograde DiI labeling from its developing target muscle (Fig. 1G-I). Imaging from pupae expressing the AP-1 nls-GFP reporter revealed the first detectable AP-1 transcriptional activity in MN5 at pupal stage P5 early (Fig. 1G), followed by continuous AP-1 transcriptional activity through all stages of dendritic growth (Fig. 1H,I, white arrows).

AP-1 is necessary for normal MN5 dendritic growth and operates downstream of neural activity

To test whether AP-1 increased MN5 dendritic growth in the absence of increased firing, we overexpressed AP-1 (UAS-*fos*; UAS-*jun*) in MN5 under the control of D42-GAL4, cha-GAL80 (see Materials and methods). Statistical comparison with controls (Fig. 2A) showed that overexpression of AP1 (Fig. 2B) caused significant increases in MN5 total dendritic length (TDL) and in the number of dendritic branches (Fig. 2D; $P \leq 0.05$, ANOVA), but the length and radii of individual dendritic segments were not affected (Fig. 2D). Dendritic territory borders were also not affected, as indicated by normal average distances of the branches

to their origin (Fig. 2D). Similar results were obtained when AP-1 was overexpressed using the motoneuron driver P103.3-GAL4 (Consoulas et al., 2002) (Fig. 2C-F). Sholl analysis (Fig. 2E) revealed that AP-1-dependent dendritic overgrowth was not restricted to specific dendritic territories. Quantitatively, AP-1 overexpression mimicked increases in MN5 dendritic branch number and TDL as induced by EKI expression (Fig. 2F).

Conversely, inhibition of AP-1 by expression of UAS-Jbz, a dominant-negative form of Jun (Sanyal et al., 2002), reduced the number of dendritic branches and TDL significantly (Fig. 2F,G). Co-expression of EKI and Jbz in MN5 significantly reduced TDL and number of dendritic branches (Fig. 2F,H), indicating that AP-1 acted downstream of activity. And finally, in Dα7 nAChR null mutants, in which excitatory cholinergic drive to MN5 is strongly reduced (Fayyazuddin et al., 2006), dendritic growth was significantly reduced (Fig. 2F,I). Although additional indirect effects via other network components cannot be ruled out entirely, the Dα7 nAChR subunit is predominantly expressed in the few neurons of the escape circuit (Fayyazuddin et al., 2006). In addition, loss of Dα7 function causes reduced AP-1 transcriptional activity in MN5 (see below). Taken together, these data indicate that both excitatory synaptic drive through nAChRs and AP-1 were necessary for normal MN5 dendrite formation, and that AP-1 affected MN5 dendritic growth downstream of activity.

AP-1-dependent gene transcription is upregulated by increased neural activity during development

We employed our newly generated AP-1 reporter to test whether increased activity affected AP-1-dependent transcription. MN5 was identified by retrograde DiI labeling (Fig. 3A,B) because many neurons in the VNC showed AP-1 reporter-mediated nuclear GFP expression (Fig. 3A,C). Following different manipulations of MN5 activity, nuclear GFP fluorescence in MN5 was live-imaged *in situ* in the intact CNS with a cooled CCD camera. First, we tested reporter sensitivity to experimental perturbations of AP-1. Inhibition of AP-1 in MN5 by expression of Jbz decreased reporter
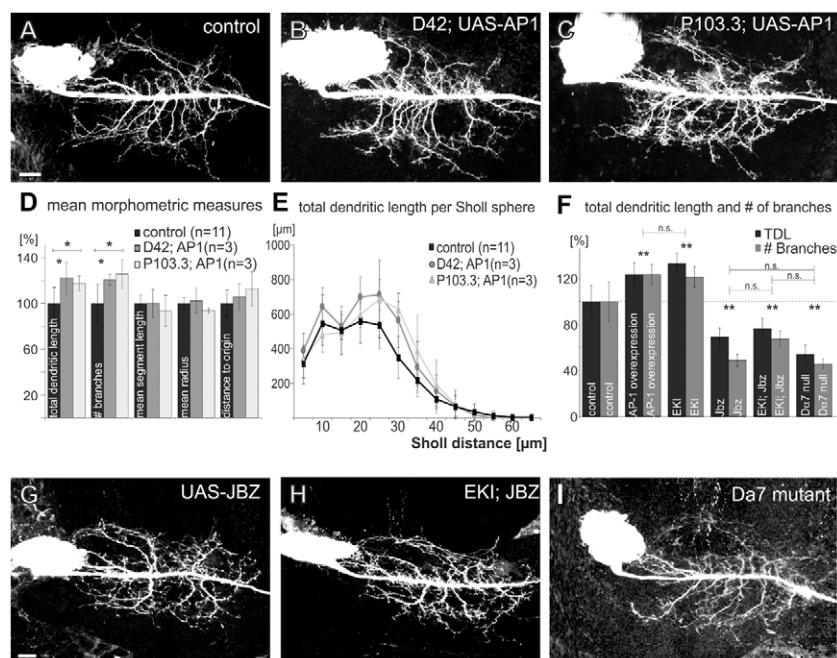
Fig. 2. Overexpression of AP-1 in MN5 under the control of D42-GAL4 or P103.3-GAL4 causes dendritic overgrowth. (**A-C**) MN5 dendritic structure in a representative control fly (A) and following expression of AP-1 (UAS-*fos*; UAS-*jun*) under the control of D42-GAL4 (B), or P103.3-GAL4 (C). (**D**) Means and s.d. normalized to mean control values of MN5 dendritic structure measures in controls (black bars) and following AP-1 overexpression (D42, dark gray; P103.3, light gray). Asterisks indicate statistically significant differences (ANOVA, *P*<0.05). (**E**) Sholl analysis of dendritic length (spheres as air distances to the origin) in controls (black squares) and following overexpression of AP-1 under the control of D42 (gray circles) and P103.3 (gray triangles). (**F**) Average and s.d. normalized to mean control of total dendritic length (black bars) and number of branches (gray bars) in controls, following overexpression of AP-1, EKI, Jbz, EKI and Jbz, and in Dα7 nAChR null mutants. Asterisks indicate statistical significant differences from control (**P*<0.01, ANOVA with Newman Keuls post-hoc testing). (**G-I**) Representative intracellular fills of MN5 from three different experimental groups: expression of Jbz (G), co-expression of Jbz and EKI (H), Dα7 nAChR null mutant (I). Scale bars: 10 µm.

fluorescence by 50%, whereas overexpression of AP-1 (UAS-*fos*, UAS-*jun*) resulted in a threefold increase of reporter fluorescence in MN5 nuclei (Fig. 3D). This confirmed that our reporter detected differences in AP-1-dependent transcription as caused by genetic manipulations of AP-1 that affected MN5 dendritic growth (Fig. 2). Second, we compared a modified reporter that contains the same minimal *elav* promoter (see Materials and methods), but the AP-1 binding sites were changed to canonical CREs by insertion of a single G (TGACTCA to TGAC**G**TCA). CRE reporter-mediated fluorescence was not altered by TrpA1-induced activity in MN5 (supplementary material Fig. S1). This confirmed that neuronal activity-driven expression of nls-GFP from our AP-1 reporter was specifically due to AP-1 activity, but not caused by non-specific activation from the minimal *elav* element.

Next, we manipulated MN5 firing activity at different periods of adult or pupal life. This was achieved through expression of the temperature-sensitive cation channel TrpA1. Current clamp recordings of MN5 confirmed that temperature shifts from 22°C to 27°C evoked tonic firing between 20 and 50 Hz (supplementary material Fig. S2), as previously reported for larval *Drosophila* motoneurons (Pulver et al., 2009). In all experiments, the temperature was maintained at 20°C during embryonic and larval development in order to avoid TrpA1 channel activation.

Induction of MN5 firing activity during pupal life caused significant increases in AP-1-dependent nls-GFP transcription. TrpA1 channel activation between pupal stage P5 and adulthood, or between P9 and adulthood, caused statistically significant increases in nls-GFP fluorescence in acutely dissected adult animals (Fig. 3E; *P*≤0.05, ANOVA with Newman Keuls post-hoc testing). No differences in nls-GFP fluorescence of MN5 nuclei were detected in controls for temperature (flies without UAS-TrpA1 reared at 29°C), flies with TrpA1 expression but no activation, and adult flies that had been exposed to TrpA1 activation between pupal stages P1 and P5 (Fig. 3E). Representative examples of nls-GFP fluorescence intensity in MN5 nuclei in three different experimental groups are depicted as pseudocolor heat maps in Fig. 3G-I.

By contrast, AP-1 activity was not increased by MN5 firing in adult flies. In semi-intact adult flies, AP-1 reporter fluorescence remained unchanged after 20 minutes of MN5 tonic firing (Fig. 3F). Because we could not accurately measure the duration between AP-1 activation and GFP reporter fluorescence, we repeated imaging every 20 minutes for a total duration of 4 hours, but did not detect increased reporter fluorescence following tonic MN5 firing (not shown). We conducted live-cell imaging of MN5 nuclear GFP fluorescence intensity in adult animals while shifting the bath temperature from 20°C to 29°C for different durations (1, 10, 30, 60, 120, 600 minutes). In no case did we observe an increase in GFP fluorescence intensity (data not shown). To account for the possibility that our semi-intact preparation did not reflect the physiological state of the intact animal, we transferred intact adult flies to 29°C for different durations and imaged AP-1 reporter fluorescence in acutely dissected animals. Nuclear GFP fluorescence intensities were similar in controls and following TrpA1 activation for 24 hours, 72 hours or 96 hours (Fig. 3F). This indicated that increased firing activity of the adult MN5 did not induce detectable increases in AP-1-dependent transcription.

CaMKII activity is upstream of AP-1-dependent transcription

Previous studies on cultured larval motoneurons indicated that activity-dependent calcium influx was required for AP-1 activation (Hartwig et al., 2008). Dα7 nicotinic AChRs are highly permeable to calcium (Séguéla et al., 1993) and are required for normal dendrite growth of MN5 (Fig. 2F,I). We utilized the AP-1 reporter to test whether CaMKII activity was necessary and/or sufficient for AP-1 activation. AP-1 reporter fluorescence in adult MN5 nuclei was live-imaged following various genetic manipulations (Fig. 4). All data were normalized to fluorescence levels in controls. Inhibition of AP-1 by expression of UAS-Jbz in MN5, inhibition of CaMKII by expression of ala (Wang et al., 1994), and Dα7 nAChR mutants all showed a significant decrease of AP-1 activity by ~50% (Fig. 4). Heterozygous mutant animals with one copy of Dα7 nAChR showed a slight but non-significant decrease in
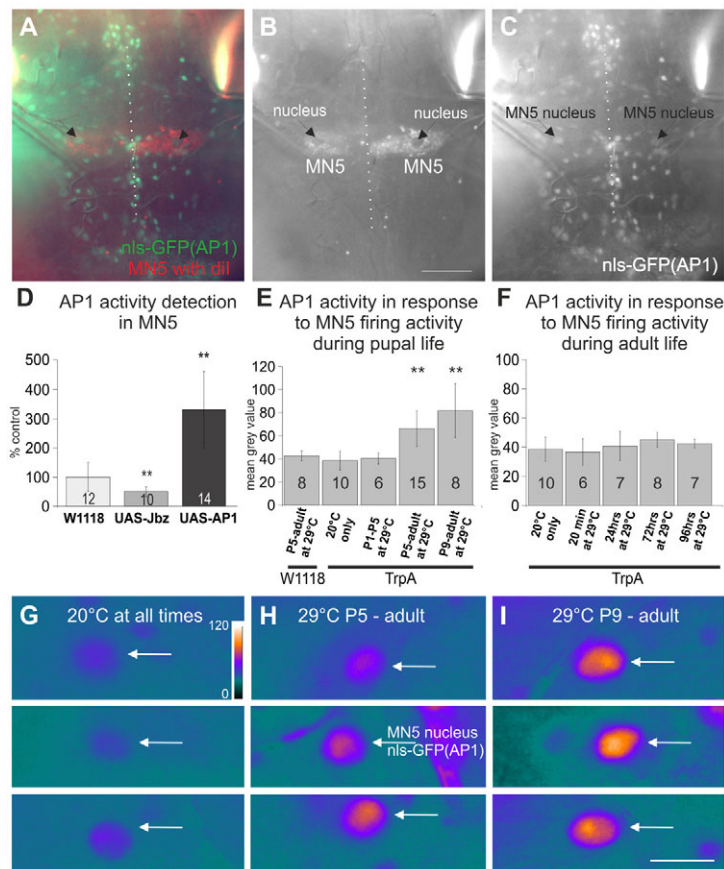
Fig. 3. AP-1-dependent transcription is increased by firing activity in the developing but not in the mature MN5. (**A-C**) Identification of MN5 in flies expressing an AP-1 reporter in all neurons. MN5 somata (A, red; B) are labeled retrogradely with DiI. Many cells in the adult VNC reveal AP-1 reporter-mediated nuclear GFP localization (A, green; C). MN5 nuclei were devoid of DiI label (A,B, black arrowheads), but showed AP-1 reporter-induced nls-GFP label (C, black arrowheads). (**D**) Quantification of fluorescence intensities in adult MN5 nuclei in controls (C380-GAL4 × w^{1118}; white bar), following expression of Jbz (gray bar) and of AP-1 (black bar, C380-GAL4 × UAS-*fos*;UAS-*jun*). **$P≤0.01$. (**E,F**) Quantification of fluorescence intensities in adult MN5 nuclei following TrpA1 channel activation (C380-GAL4; AP-1 nls-GFP/UAS-TrpA1) for different durations either during specific periods of pupal development (E; **$P≤0.01$, ANOVA with Newman Keuls post-hoc testing), or during adult life (F). (**G-I**) Three representative examples each for three experimental groups of live images of AP-1 reporter-induced nls-GFP signal in MN5 nuclei (white arrows) depicted as pseudocolor heat maps (see color scale bar). (G) Animals on 20°C at all times. (H) Animals raised at 20°C until P5 and shifted to 29°C until image acquisition in the adult. (I) Animals raised at 20°C until P9 and then shifted to 29°C until image acquisition in the adult. Error bars represent s.d. Scale bars: 40 μm (A-C); 10 μm (G-I).

reporter fluorescence (Fig. 4). By contrast, expression of a constitutively active form of CaMKII in MN5 (CaMKII T287D) (Jin et al., 1998; Wang et al., 1998) caused a significant increase in AP-1 reporter fluorescence, both in MN5 with normal Dα7 nAChRs and in Dα7 nAChR null mutants (Fig. 4). This indicated that CaMKII was downstream of calcium influx through Dα7 nAChRs and upstream of AP-1.

Overexpression of AP-1 in MN5 can also inhibit dendrite growth

Paradoxically, expression of AP-1 under the control of a third motoneuron driver, C380-GAL4 (Budnik et al., 1996), caused significant reductions in the number of dendritic branches and TDL (Fig. 5A-D). MN5 dendrites did not reach the normal neuropil boundaries and appeared less ramified with several parts missing (Fig. 5B,D). Quantitatively, TDL and the number of branches were decreased by nearly 50% (Fig. 5E; $P≤0.05$, unpaired *t*-test). Neither the mean length nor the average radii of the remaining dendritic branches was affected (Fig. 5E). Overlays of two representative dendrite reconstructions in controls (Fig. 5C) and following AP-1 overexpression under the control of C380-GAL4 (Fig. 5D; *n*=12) indicated that the most severe dendritic defects were in the proximal-posterior region (Fig. 5D, arrowhead). In addition to C380, we used Dα7 nAChR-GAL4 (Fayyazuddin et al., 2006) as a fourth driver to express AP-1 in MN5. Similar to C380-GAL4 (Fig. 5B,D), expression of AP-1 under the control of Dα7 nAChR-GAL4 caused a significant reduction in the number of adult MN5 dendrites. Dendritic defects as induced by AP-1 expression under the control of C380-GAL4 or Dα7 nAChR-GAL4 were not caused by a loss of previously grown branches, but, instead, MN5 already contained

fewer dendrites during the early stages of dendritic growth (supplementary material Fig. S3). Finally, overexpression of either *fos* (Fig. 5G) or *jun* alone (Fig. 5H) did not phenocopy the dendritic defects caused by AP-1 expression under the control of C380. This supported the idea that reduced MN5 dendritic branching was also due to transcriptional activity of the AP-1 heterodimer.

Overexpression of AP-1 during early stages inhibits dendritic growth

What might be the explanation for the unexpected observation that different GAL4 drivers result in opposite phenotypes when they are used to overexpress AP-1 in MN5? First, different expression levels might cause different downstream consequences. Second, different GAL4 drivers might express at different times during pupal life. We analyzed the timing of expression during pupal life in D42-GAL4, P103.3-GAL4 and C380-GAL4 animals with a UAS-mCD8-GFP reporter. Although P103.3- and D42-driven GFP expression was seen in other cells at early stages, GFP expression in MN5 was first detectable at ~25 hours APF (supplementary material Fig. S4; Fig. 6C,D). By contrast, C380 already showed robust expression in MN5 at early pupal stage P5 (supplementary material Fig. S4; 12.5 hours APF), before the start of MN5 dendritic growth (Fig. 1A; Fig. 6F). Similarly, immunocytochemistry for Dα7 nAChRs indicated that this driver also expressed at P5 (see below). By contrast, P103.3 and D42 turned on at pupal stage P6 when primary dendrites of MN5 were already present (Fig. 1B; Fig. 6A). Therefore, using C380 and Dα7 caused AP-1 expression before the start of dendritic growth and inhibited new dendritic branch formation, whereas D42 and P103.3 caused AP-1 expression at later stages and promoted dendrite growth.
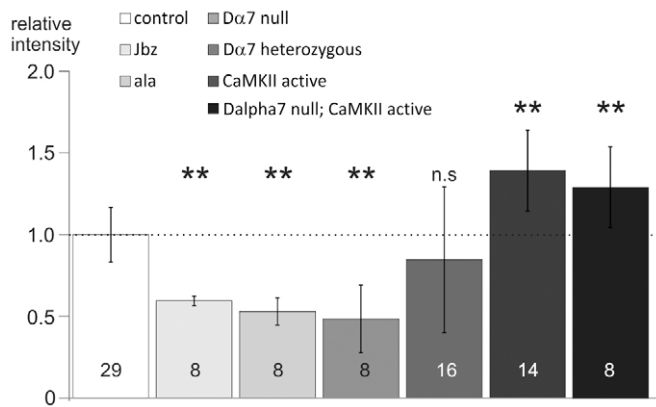
Fig. 4. CaMKII is upstream of AP-1. Means and s.d. of AP-1 reporter fluorescence intensities in adult MN5 nuclei normalized to controls (dotted line). Bars from left to right: control, inhibition of AP-1 (by Jbz), inhibition of CaMKII (by ala), homozygous Dα7 nAChR mutants, heterozygous Dα7 nAChR mutants, expression of constitutively active CaMKII in a control or in a Dα7 nAChR null background (**$P \leq 0.01$, ANOVA with Newman Keuls post-hoc testing). n.s., not significant.

Fig. 5. Overexpression of AP-1 in MN5 under the control of C380-GAL4 causes reduced dendritic branching. (**A,B**) Representative projection views of MN5 dendritic structure in a control fly (A) and following expression of AP-1 (UAS-*fos*; UAS-*jun*) under the control C380-GAL4 (B). (**C,D**) Overlay of two representative dendrite reconstructions (C, control; D, C380-driven AP-1 expression). Arrowheads in A-D indicate characteristic dendritic region that was missing following AP-1 overexpression in MN5. (**E**) Quantification of MN5 dendritic structure in controls (black bars) compared with C380-driven AP-1 overexpression (gray bars). Values were normalized to mean control values (*$P < 0.05$, unpaired *t*-test). (**F**) Representative image of MN5 following expression of AP-1 under the control of Dα7 nAChR-GAL4. (**G,H**) MN5 dendritic structure following overexpression of either UAS-*fos* (G) or UAS-*jun* (H) alone under the control of C380-GAL4 shows no obvious defect. Scale bar: 10 μm.

To investigate further whether AP-1 expression timing was key to either promotion or inhibition of dendrite growth, we used temporal and regional gene expression targeting (TARGET) (McGuire et al., 2003). We included the temperature-sensitive GAL4 inhibitor GAL80 under the control of a strong promoter (TubP-GAL80^ts) in flies expressing AP-1 under the control of C380-GAL4. In these flies, the timing of AP-1 overexpression was delayed by relieving GAL80 repression of GAL4 by a temperature shift to 30°C at pupal stage P6. We tested the validity of this technique by using UAS-GFP as a reporter of GAL4 activity before and after the temperature shift. No detectable GFP expression was found in animals raised at 25°C (*n*=5). Following a temperature shift from 25°C to 30°C at P6, GFP expression in the VNC and in MN5 was first detectable after 12 hours. However, compared with normal C380-GAL4-driven GFP expression in MN5, fluorescence was fainter and was restricted to the soma and primary neurite between pupal stages 6 and 9. This might be caused by residual GAL80 or by slow accumulation and folding of GFP following the temperature shift. Although temperature-induced release of GAL80 suppression does not allow a precise temporal shift of C380 expression into the timing of D42 expression, it does effectively postpone the onset of GAL4-mediated transgene expression in C380 flies to later pupal stages (Fig. 6G).

C380-GAL4-driven expression of AP-1 without GAL80 suppression resulted in significantly fewer dendritic branches (Fig. 5B,E; Fig. 6H), but shifting expression past pupal stage P6 prevented obvious dendritic defects (Fig. 6G,I,J). All 12 animals with normal C380-GAL4-driven expression of AP-1 showed a lack of all proximal posterior dendrites (Fig. 5D, white arrowhead), whereas all animals with GAL80 suppression until pupal stage P6 (Fig. 6I; *n*=7) or until pupal stage P9 (Fig. 6J; *n*=4) showed elaborate MN5 dendrites throughout all regions of the tree.

Increased neural activity before the onset of dendritic development also leads to dendritic defects

If AP-1 is induced by neural activity in MN5, then the effect of early AP-1 expression should be mimicked by a premature increase in activity. Therefore, we tested whether increased activity before
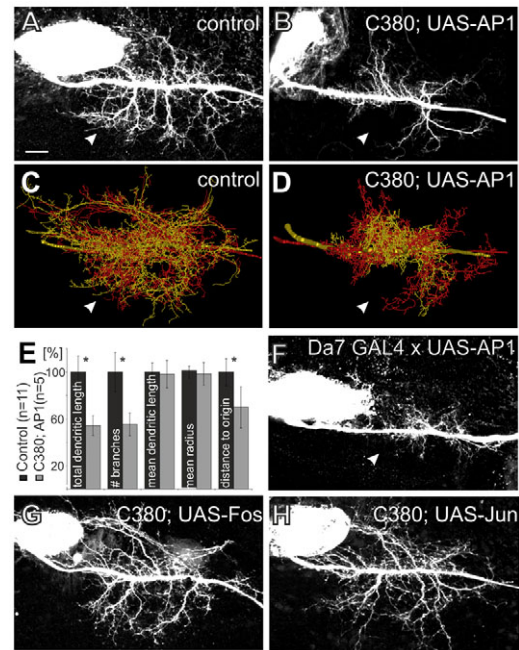
the onset of dendritic growth also disrupted dendrite growth. UAS-TrpA1 was expressed in MN5 under the control of C380-GAL4 and activated by temperature shifts either between pupal stages P2 and P6 (*n*=6) or between P2 and P9 (*n*=5). Induced premature activity severely reduced the size and complexity of the MN5 dendrite (Fig. 7B,C). In all 11 preparations, MN5 was lacking multiple dendritic sub-trees (Vonhoff and Duch, 2010), and neither posterior nor anterior dendrites reached their normal territory boundaries. Dendritic defects as induced by premature activity (Fig. 7B,C) were rescued by expression of a dominant-negative form of an AP-1 subunit (Fig. 7D). In all five animals tested, MN5 showed normal numbers of dendritic sub-trees, and posterior and anterior dendrites reached their normal territory boundaries. Control flies without the TrpA1 transgene that were raised under the same temperature conditions did not show any obvious dendritic defect (*n*=6; data not shown). TrpA1 activation in MN5 at later pupal stages, when first order dendritic branches had already formed, did not induce any obvious dendritic defect (from P6 to P9; *n*=7; Fig. 7A). Therefore, both increased neural activity and AP-1 overexpression before pupal stage P6 impaired dendrite development. By contrast, increased MN5 activity (Duch et al., 2008) and AP-1 overexpression after pupal stage P6 promoted dendritic branching.
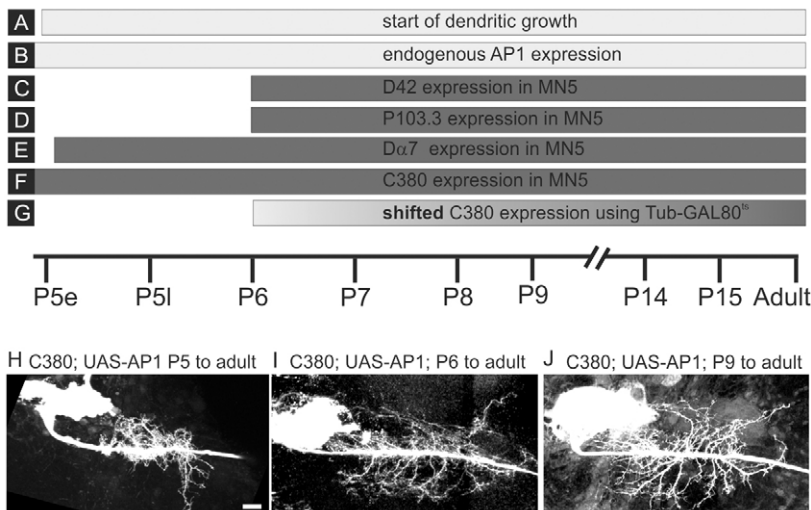
Fig. 6. The timing of AP-1 overexpression during *Drosophila* development determines whether dendritic growth is reduced or promoted. (**A-G**) Bars denote the timing of relevant developmental events and expression of various GAL4 drivers during pupal life. P5e, 5 early; P5l, P5 late. (**H-J**) Representative projection views of MN5 dendritic structure following AP-1 overexpression with C380-GAL4, Tub-GAL80[ts] without temperature shift (H), and following restriction of expression to stages older than P6 (I) or to stages older than P9 (J). Scale bar: 10 μm.

Expression of AChRs precedes onset of MN5 dendritic growth

It was technically prohibitively challenging to record MN5 activity during normal pupal development *in vivo*. However, current clamp recordings from dissected pupae revealed that MN5 fired action potentials upon current injection during stages of dendritic growth (data not shown), similar to the MN5 homolog in the moth *Manduca sexta* (Duch and Levine, 2000). Acetylcholine is the most abundant excitatory neurotransmitter in the fly central nervous
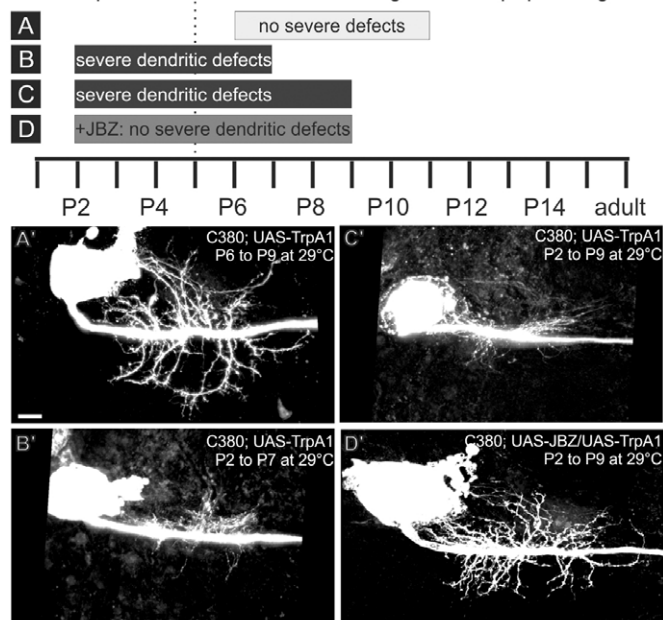

Fig. 7. Induction of premature MN5 activity causes dendritic defects. (**A-D′**) Induction of MN5 firing activity via TrpA1 channel activation during specific times of pupal development. Dotted line indicates onset of dendritic growth. C380-GAL4; UAS-TrpA1 flies were transferred to 29°C between pupal stages P6 and P9 (A,A′), between P2 and P7 (B,B′), and between P2 and P9 (C,C′). Inhibition of AP-1 by expression of UAS-Jbz rescued dendritic defects as induced by imposed premature activity (D,D′). Scale bar: 10 μm.

system, and MN5 receives excitatory synaptic drive to the Dα7 nAChRs (Fayyazuddin et al., 2006), thus yielding the timing of Dα7 nAChR expression in MN5 a useful indicator for potential increases in MN5 activity during normal pupal life. Immunolabeling of Dα7 nAChRs (Fig. 8, magenta) was paired with anti-GFP labeling in flies expressing GFP under the control of C380-GAL4 to identify motoneurons (Fig. 8, green). During the last larval stage (third instar larvae, L3) and the first pupal stage (P1, 2 hours AFP) Dα7 nAChRs were abundantly expressed throughout the VNC (Fig. 8A,B). The level of Dα7 nAChR expression decreased at pupal stage P2 (4 hours APF; Fig. 8C). Remarkably, Dα7 nAChRs were undetectable between pupal stages P3 and early P5 (Fig. 8D-F; 8-12.5 hours APF). Interestingly, at pupal stage mid P5 (15 hours APF), just 2.5 hours after the onset of MN5 dendritic growth, Dα7 nAChR expression was clearly detected in MN5 and other neurons in the VNC (Fig. 8G) and remained through adulthood (Fig. 8G-L). This is consistent with the idea that AP-1-mediated dendritic defects would not be induced by activity during normal development, because excitatory synaptic transmission to MN5 was present only at pupal stages, when activity and AP-1 were found to promote dendritic branching.

DISCUSSION

By combining genetic and neuroanatomical tools with imaging in a single-cell model, the adult MN5 in *Drosophila*, this study demonstrates that: (1) AP-1 is transcriptionally active during all stages of postembryonic motoneuron dendritic growth, (2) AP-1 and excitatory cholinergic inputs are required for normal dendrite growth in MN5, (3) AP-1 transcriptional activity is enhanced via a CaMKII-dependent mechanism by increased neural activity during pupal development but not in the adult, and (4) both activity and AP-1 can promote or inhibit dendritic branching, depending on the developmental stage.

AP-1 is required for normal MN5 dendrite growth downstream of activity and CaMKII

Although AP-1 has been thought to regulate dendrite development in an activity-dependent manner via global changes in gene expression, probably in a calcium-dependent manner as described for CREB or Crest (Redmond et al., 2002; West and Greenberg, 2011; Aizawa et al., 2004), direct evidence for this hypothesis was sparse.
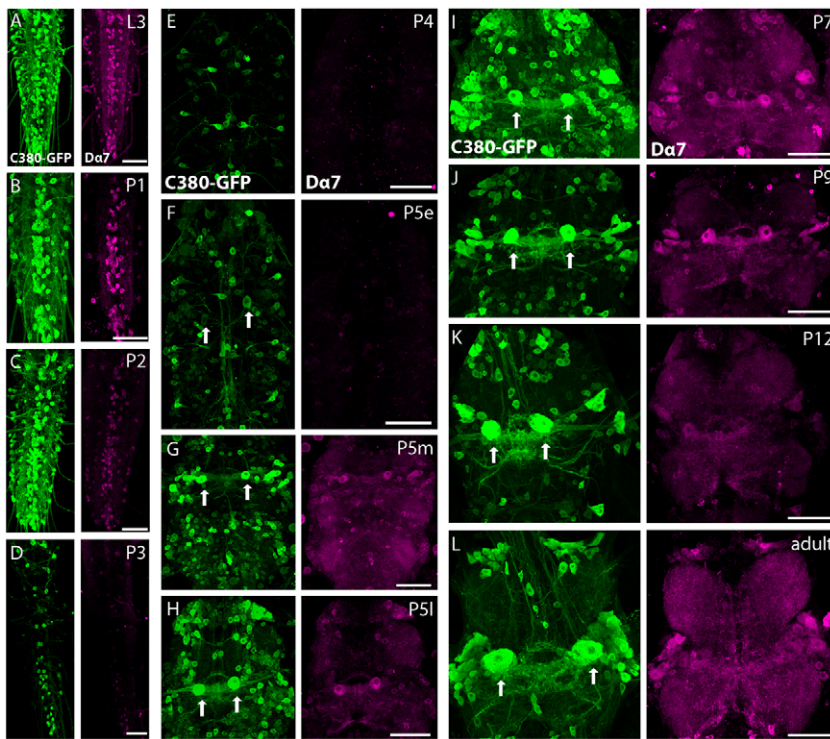
Fig. 8. Developmental changes of the expression of Dα7 nAChRs in the *Drosophila* thoracic ventral nerve cord (VNC). Overviews of the thoracic VNC following Dα7 nAChR (right, magenta) and GFP immunocytochemistry in flies expressing UAS-mCD8-GFP under the control of C380-GAL4 (left, green) at different pupal stages. (**A**) L3: third instar larvae. (**B**) P1: ~1 hour APF. (**C**) P2: ~3 hours APF. (**D**) P3: ~6 hours APF. (**E**) P4: ~8 hours APF. (**F**) early P5 (P5e): ~12.5 hours APF. (**G**) mid P5 (P5m): ~15 hours APF. (**H**) late P5 (P5l): ~18 hours APF. (**I**) P7: ~40 hours APF. (**J**) P9: ~70 hours APF. (**K**) P12: ~75 hours APF. (**L**) Adult. White arrows point to MN5 somata at stages when it could be unambiguously identified. Scale bars: 50 μm.

This study demonstrated that excitatory cholinergic input to MN5 and AP-1 transcriptional activity were required for normal dendrite growth of MN5 during pupal life. MN5 total dendritic length and branch numbers were significantly reduced (~50%) by inhibition of AP-1 (by Jbz expression) and in Dα7 nAChR mutants. Conversely, overexpression of AP-1 or increased MN5 excitability as induced by potassium channel knockdown (by EKI) (Duch et al., 2008) increased dendritic branching. Clearly, AP-1 acted downstream of activity as inhibition of AP-1 by Jbz completely attenuated EKI-mediated dendritic growth and branching.

A new AP-1 reporter was employed to measure activity-induced AP-1 transcriptional activity by imaging, and to gain insight into the pathway that might connect MN5 activity to AP-1-dependent transcription. Although the detection threshold of this reporter might be too low to detect small changes in AP-1 activity, sensitivity was sufficient to reliably report increased AP-1 activity following overexpression of *fos* and *jun*, inhibition of AP-1 transcriptional activity by Jbz expression, and changes in AP-1 activity as induced by various manipulations of cellular signaling. Therefore, the reporter was deemed suitable for testing changes in AP-1 transcriptional activity in MN5.

Targeted expression of TrpA1 channels in MN5 allowed the induction of firing *in vivo* by temperature shifts during selected developmental periods. Activation of MN5 during pupal life for 36 hours (P9 to adult) or longer (P5 to adult) caused significant increases in AP-1-induced nuclear GFP fluorescence. By contrast, in adults neither similar nor longer durations of TrpA1 activation resulted in any detectable increase in AP-1 reporter-mediated nuclear GFP fluorescence in MN5. Similarly, live imaging in semi-intact adult preparations did not reveal any detectable AP-1 activity upon acute TrpA1 activation for various durations. This indicated that activity-dependent AP-1 activation was restricted to pupal life. However, we did not test whether AP-1 activation in the adult MN5 occurred upon patterned activity. Spaced stimuli that reflect endogenous activity patterns

are required for insect motoneuron axonal (Duch and Mentel, 2003; Carrillo et al., 2010) and dendritic (Crisp et al., 2011) development and can regulate mammalian neuron dendritic morphology (Wu et al., 2001). However, during flight, MN5 fires tonically at frequencies between 5 and 20 Hz (Koenig and Ikeda, 1980a; Koenig and Ikeda, 1980b; Levine and Wyman, 1973), a pattern that is well reflected by temperature-controlled TrpA1 channel activation (Pulver et al., 2009). Therefore, adult flight behavior is unlikely to induce AP-1 activity, which is involved in dendrite and synapse development (Freeman et al., 2010). This is consistent with the assumption that dendritic structure is fairly stable in the adult (Mizrahi and Katz, 2003; Zuo et al., 2005).

cAMP and Jun N-terminal kinase (Jnk) have been implicated as potential links between activity and AP-1 activation (Sanyal et al., 2002). Cell culture studies on *Drosophila* larval motoneurons and giant neurons demonstrate a role of calcium (Peng et al., 2007; Hartwig et al., 2008). We showed that Dα7 nAChRs, which are highly permeable to calcium (Séguéla et al., 1993; Oliveira et al., 2010), were required for normal MN5 dendritic growth. Combining genetic manipulation of Dα7 nAChRs, AP-1 and CaMKII with imaging of AP-1 reporter activity revealed that CaMKII was required downstream of Dα7 nAChRs to cause AP-1-dependent transcription. These data show that activity-dependent calcium influx through nAChRs might activate AP-1 during pupal life via a CaMKII-dependent mechanism *in vivo*.

Activity and AP-1 can promote or inhibit dendritic growth during pupal life, depending on timing

In larval motoneurons, AP-1 is required for dendritic overgrowth as induced by artificially increased activity (Hartwig et al., 2008). In MN5, AP-1 is required downstream of nAChRs and CaMKII for normal dendritic growth. By contrast, premature expression of AP-1 in MN5 inhibited dendritic growth. Our data were consistent with the hypothesis that timing is the crucial factor. First, P103.3 and

D42 both caused similar overgrowth but exhibited fairly different expression patterns. Second, C380-GAL4 and Dα7 nAChR-GAL4 both inhibited MN5 dendrite growth but expressed in largely different sets of neurons. Therefore, the common factor of C380 and Dα7 nAChR on the one hand and D42 and P103.3 on the other hand was timing. Third, shifting the timing of C380-GAL4-driven AP-1 expression to later stages prevented dendritic defects. Fourth, imposed activity prior to P5 by TrpA1 activation also inhibited dendritic branching. Dendritic defects as induced by imposed premature activity were rescued by inhibition of AP-1 via Jbz expression in MN5.

A model for the roles of cholinergic synapses, early developmental activity, and AP-1 in normal dendrite development during pupal life

MN5 early dendritic growth starts at early pupal stage 5 (P5), and expression of Dα7 nAChRs begins 2.5 hours later, at mid stage P5 (Fig. 9). Similarly, *Xenopus* optic tectal and turtle cortical neurons receive glutamatergic and GABAergic inputs as soon as the first dendrites are formed (Wu et al., 1996; Blanton and Kriegstein, 1991). In vertebrates, early synaptic inputs and neurotransmitters play essential roles in dendrite development (Bestman et al., 2008). Our data are consistent with the hypothesis that the endogenous expression of nAChRs caused increased activity throughout the developing motor networks, which, in turn, upregulated AP-1-dependent transcription and dendritic growth via a CaMKII-dependent mechanism (Fig. 9). During zebrafish spinal cord development, activity is required for strengthening functional central pattern generator (CPG) connectivity (Warp et al., 2012). As dendrites are the seats of input synapses to motoneurons, an activity-dependent component in motoneuron dendritic growth that follows early synaptogenesis might function to refine dendrite shape during the integration into the developing CPG.

Conversely, overexpression of AP-1 before MN5 receives excitatory cholinergic input disrupted new dendritic branch formation. A possible explanation for the opposite effects of AP-1 activity at different stages might result from the mode of action of downstream targets of AP-1. New dendritic branch formation may be promoted by increased filopodia motility, but highly motile filopodia are also prone to retraction and collapse. In multiple

systems, synaptic input stabilizes newly formed dendritic filopodia (Cline, 2001; Sin et al., 2002; Van Aelst and Cline, 2004; Niell et al., 2004). In embryonic *Drosophila* motoneurons, cholinergic input stabilizes newly formed dendritic branches (Tripodi et al., 2008). If downstream targets of AP-1 promoted dendritic filopodia motility, these might be exclusively stabilized by cholinergic synaptic transmission at pupal stages P6 and later, but not before P6. Although this could explain the opposite effects of AP-1 on dendritic growth before and after cholinergic synapse formation, future studies will be needed to identify transcriptional targets of AP-1 to satisfactorily test this hypothesis.

Competing interests statement
The authors declare no competing financial interests.

Supplementary material
Supplementary material available online at
http://dev.biologists.org/lookup/suppl/doi:10.1242/dev.089235/-/DC1

References
Aizawa, H., Hu, S. C., Bobb, K., Balakrishnan, K., Ince, G., Gurevich, I., Cowan, M. and Ghosh, A. (2004). Dendrite development regulated by CREST, a calcium-regulated transcriptional activator. *Science* **303**, 197-202.
Barolo, S. and Posakony, J. W. (2002). Three habits of highly effective signaling pathways: principles of transcriptional control by developmental cell signaling. *Genes Dev.* **16**, 1167-1181.
Barolo, S., Carver, L. A. and Posakony, J. W. (2000). GFP and beta-galactosidase transformation vectors for promoter/enhancer analysis in Drosophila. *Biotechniques* **29**, 726-732.
Bestman, J., Santos da Silva, J. and Cline, H. (2008). Dendrite development. In: *Dendrites* (ed. G. Stuart, N. Spruston, M. Hausser), pp 69–94. Oxford, UK: Oxford University Press.
Blanton, M. G. and Kriegstein, A. R. (1991). Spontaneous action potential activity and synaptic currents in the embryonic turtle cerebral cortex. *J. Neurosci.* **11**, 3907-3923.
Boerner, J. and Duch, C. (2010). Average shape standard atlas for the adult Drosophila ventral nerve cord. *J. Comp. Neurol.* **518**, 2437-2455.
Brierley, D. J., Blanc, E., Reddy, O. V., Vijayraghavan, K. and Williams, D. W. (2009). Dendritic targeting in the leg neuropil of Drosophila: the role of midline signalling molecules in generating a myotopic map. *PLoS Biol.* **7**, e1000199.
Budnik, V., Koh, Y. H., Guan, B., Hartmann, B., Hough, C., Woods, D. and Gorczyca, M. (1996). Regulation of synapse structure and function by the Drosophila tumor suppressor gene dlg. *Neuron* **17**, 627-640.
Carrillo, R. A., Olsen, D.P., Yoon, K. S. and Keshishian H. (2012). Presynaptic activity and CaMKII modulate retrograde semaphorin signaling and synaptic refinement. *Neuron* **68**, 32-44.
Chen, Y. and Ghosh, A. (2005). Regulation of dendritic development by neuronal activity. *J. Neurobiol.* **64**, 4-10.
Cline, H. T. (2001). Dendritic arbor development and synaptogenesis. *Curr. Opin. Neurobiol.* **11**, 118-126.
Coggshall, J. C. (1978). Neurons associated with the dorsal longtitudinal flight muscles of Drosophilla melanogaster. *J. Comp. Neurol.* **177**, 707-720.
Consoulas, C., Restifo, L. L. and Levine, R. B. (2002). Dendritic remodeling and growth of motoneurons during metamorphosis of Drosophila melanogaster. *J. Neurosci.* **22**, 4906-4917.
Corty, M. M., Matthews, B. J. and Grueber, W. B. (2009). Molecules and mechanisms of dendrite development in Drosophila. *Development* **136**, 1049-1061.
Crisp, S. J., Evers, J. F. and Bate, M. (2011). Endogenous patterns of activity are required for the maturation of a motor network. *J. Neurosci.* **31**, 10445-10450.
Curran, T. and Franza, B. R., Jr (1988). Fos and Jun: the AP-1 connection. *Cell* **55**, 395-397.
Duch, C. and Levine, R. B. (2000). Remodeling of membrane properties and dendritic architecture accompanies the postembryonic conversion of a slow into a fast motoneuron. *J. Neurosci.* **20**, 6950-6961.
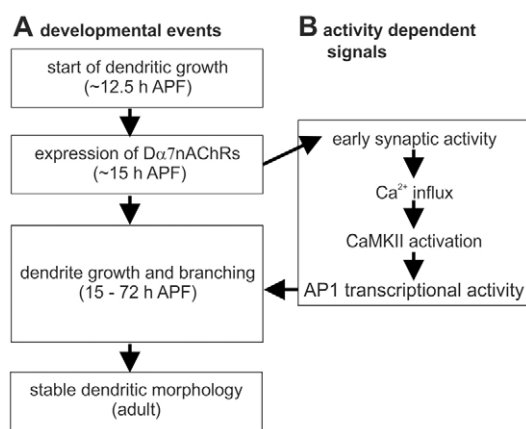

Fig. 9. A model of the roles of nAChRs, early activity, CaMKII and AP-1 in activity-dependent dendrite growth of a *Drosophila* motoneuron during normal postembryonic development. (**A**) The timing of developmental events. (**B**) Summary of the roles of cholinergic input, CaMKII and AP-1 that were found to occur in MN5.

Duch, C. and Mentel, T. (2003). Stage-specific activity patterns affect motoneuron axonal retraction and outgrowth during the metamorphosis of Manduca sexta. *Eur. J. Neurosci.* **17**, 945-962.

Duch, C. and Mentel, T. (2004). Activity affects dendritic shape and synapse elimination during steroid controlled dendritic retraction in Manduca sexta. *J. Neurosci.* **24**, 9826-9837.

Duch, C., Vonhoff, F. and Ryglewski, S. (2008). Dendrite elongation and dendritic branching are affected separately by different forms of intrinsic motoneuron excitability. *J. Neurophysiol.* **100**, 2525-2536.

Eresh, S., Riese, J., Jackson, D. B., Bohmann, D. and Bienz, M. (1997). A CREB-binding site as a target for decapentaplegic signalling during Drosophila endoderm induction. *EMBO J.* **16**, 2014-2022.

Evers, J. F., Schmitt, S., Sibila, M. and Duch, C. (2005). Progress in functional neuroanatomy: precise automatic geometric reconstruction of neuronal morphology from confocal image stacks. *J. Neurophysiol.* **93**, 2331-2342.

Fayyazuddin, A., Zaheer, M. A., Hiesinger, P. R. and Bellen, H. J. (2006). The nicotinic acetylcholine receptor Dalpha7 is required for an escape behavior in Drosophila. *PLoS Biol.* **4**, e63.

Flavell, S. W. and Greenberg, M. E. (2008). Signaling mechanisms linking neuronal activity to gene expression and plasticity of the nervous system. *Annu. Rev. Neurosci.* **31**, 563-590.

Franciscovich, A. L., Mortimer, A. D., Freeman, A. A., Gu, J. and Sanyal, S. (2008). Overexpression screen in Drosophila identifies neuronal roles of GSK-3 beta/shaggy as a regulator of AP-1-dependent developmental plasticity. *Genetics* **180**, 2057-2071.

Freeman, A., Bowers, M., Mortimer, A. V., Timmerman, C., Roux, S., Ramaswami, M. and Sanyal, S. (2010). A new genetic model of activity-induced Ras signaling dependent pre-synaptic plasticity in Drosophila. *Brain Res.* **1326**, 15-29.

Furrer, M. P., Kim, S., Wolf, B. and Chiba, A. (2003). Robo and Frazzled/DCC mediate dendritic guidance at the CNS midline. *Nat. Neurosci.* **6**, 223-230.

Greenberg, M. E., Ziff, E. B. and Greene, L. A. (1986). Stimulation of neuronal acetylcholine receptors induces rapid gene transcription. *Science* **234**, 80-83.

Grueber, W. B., Jan, L. Y. and Jan, Y. N. (2002). Tiling of the Drosophila epidermis by multidendritic sensory neurons. *Development* **129**, 2867-2878.

Grueber, W. B., Jan, L. Y. and Jan, Y. N. (2003). Different levels of the homeodomain protein cut regulate distinct dendrite branching patterns of Drosophila multidendritic neurons. *Cell* **112**, 805-818.

Guthrie, K. M., Anderson, A. J., Leon, M. and Gall, C. (1993). Odor-induced increases in c-fos mRNA expression reveal an anatomical "unit" for odor processing in olfactory bulb. *Proc. Natl. Acad. Sci. USA* **90**, 3329-3333.

Hartwig, C. L., Worrell, J., Levine, R. B., Ramaswami, M. and Sanyal, S. (2008). Normal dendrite growth in Drosophila motor neurons requires the AP-1 transcription factor. *Dev. Neurobiol.* **68**, 1225-1242.

Hunt, S. P., Pini, A. and Evan, G. (1987). Induction of c-fos-like protein in spinal cord neurons following sensory stimulation. *Nature* **328**, 632-634.

Ikeda, K. and Koenig, J. H. (1988). Morphological identification of the motor neurons innervating the dorsal longitudinal flight muscle of Drosophila melanogaster. *J. Comp. Neurol.* **273**, 436-444.

Jefferis, G. S., Marin, E. C., Stocker, R. F. and Luo, L. (2001). Target neuron prespecification in the olfactory map of Drosophila. *Nature* **414**, 204-208.

Jin, P., Griffith, L. C. and Murphey, R. K. (1998). Presynaptic calcium/calmodulin-dependent protein kinase II regulates habituation of a simple reflex in adult Drosophila. *J. Neurosci.* **18**, 8955-8964.

Kaczmarek, L. and Chaudhuri, A. (1997). Sensory regulation of immediate-early gene expression in mammalian visual cortex: implications for functional mapping and neural plasticity. *Brain Res. Brain Res. Rev.* **23**, 237-256.

Koch, C. and Segev, I. (2000). The role of single neurons in information processing. *Nat. Neurosci.* **3 Suppl.**, 1171-1177.

Koenig, J. H. and Ikeda, K. (1980a). Neural interactions controlling timing of flight muscle activity in Drosophila. *J. Exp. Biol.* **87**, 121-136.

Koenig, J. H. and Ikeda, K. (1980b). Interspike interval relationship among flight muscle fibres in Drosophila. *J. Exp. Biol.* **87**, 137-147.

Komiyama, T. and Luo, L. (2007). Intrinsic control of precise dendritic targeting by an ensemble of transcription factors. *Curr. Biol.* **17**, 278-285.

Komiyama, T., Sweeney, L. B., Schuldiner, O., Garcia, K. C. and Luo, L. (2007). Graded expression of semaphorin-1a cell-autonomously directs dendritic targeting of olfactory projection neurons. *Cell* **128**, 399-410.

Lamph, W. W., Wamsley, P., Sassone-Corsi, P. and Verma, I. M. (1988). Induction of proto-oncogene JUN/AP-1 by serum and TPA. *Nature* **334**, 629-631.

Levine, J. D. and Wyman, R. J. (1973). Neurophysiology of flight in wild-type and a mutant Drosophila. *Proc. Natl. Acad. Sci. USA* **70**, 1050-1054.

Libersat, F. and Duch, C. (2004). Mechanisms of dendritic maturation. *Mol. Neurobiol.* **29**, 303-320.

Lohmann, C. and Wong, R. O. (2005). Regulation of dendritic growth and plasticity by local and global calcium dynamics. *Cell Calcium* **37**, 403-409.

Lohmann, C., Myhr, K. L. and Wong, R. O. (2002). Transmitter-evoked local calcium release stabilizes developing dendrites. *Nature* **418**, 177-181.

London, M. and Häusser, M. (2005). Dendritic computation. *Annu. Rev. Neurosci.* **28**, 503-532.

Mack, K. J. and Mack, P. A. (1992). Induction of transcription factors in somatosensory cortex after tactile stimulation. *Brain Res. Mol. Brain Res.* **12**, 141-147.

Mauss, A., Tripodi, M., Evers, J. F. and Landgraf, M. (2009). Midline signalling systems direct the formation of a neural map by dendritic targeting in the Drosophila motor system. *PLoS Biol.* **7**, e1000200.

McGuire, S. E., Le, P. T., Osborn, A. J., Matsumoto, K. and Davis, R. L. (2003). Spatiotemporal rescue of memory dysfunction in Drosophila. *Science* **302**, 1765-1768.

Mizrahi, A. and Katz, L. C. (2003). Dendritic stability in the adult olfactory bulb. *Nat. Neurosci.* **6**, 1201-1207.

Moore, A. W., Jan, L. Y. and Jan, Y. N. (2002). hamlet, a binary genetic switch between single- and multiple- dendrite neuron morphology. *Science* **297**, 1355-1358.

Morgan, J. I., Cohen, D. R., Hempstead, J. L. and Curran, T. (1987). Mapping patterns of c-fos expression in the central nervous system after seizure. *Science* **237**, 192-197.

Niell, C. M., Meyer, M. P. and Smith, S. J. (2004). In vivo imaging of synapse formation on a growing dendritic arbor. *Nat. Neurosci.* **7**, 254-260.

Oliveira, E. E., Pippow, A., Salgado, V. L., Büschges, A., Schmidt, J. and Kloppenburg, P. (2010). Cholinergic currents in leg motoneurons of Carausius morosus. *J. Neurophysiol.* **103**, 2770-2782.

Peng, I. F., Berke, B. A., Zhu, Y., Lee, W. H., Chen, W. and Wu, C. F. (2007). Temperature-dependent developmental plasticity of Drosophila neurons: cell-autonomous roles of membrane excitability, Ca2+ influx, and cAMP signaling. *J. Neurosci.* **27**, 12611-12622.

Pulver, S. R., Pashkovski, S. L., Hornstein, N. J., Garrity, P. A. and Griffith, L. C. (2009). Temporal dynamics of neuronal activation by Channelrhodopsin-2 and TRPA1 determine behavioral output in Drosophila larvae. *J. Neurophysiol.* **101**, 3075-3088.

Redmond, L. (2008). Translating neuronal activity into dendrite elaboration: signaling to the nucleus. *Neurosignals* **16**, 194-208.

Redmond, L., Kashani, A. H. and Ghosh, A. (2002). Calcium regulation of dendritic growth via CaM kinase IV and CREB-mediated transcription. *Neuron* **34**, 999-1010.

Ryglewski, S. and Duch, C. (2009). Shaker and Shal mediate transient calcium-independent potassium current in a Drosophila flight motoneuron. *J. Neurophysiol.* **102**, 3673-3688.

Ryglewski, S., Lance, K., Levine, R. B. and Duch, C. (2012). Ca(v)2 channels mediate low and high voltage-activated calcium currents in Drosophila motoneurons. *J. Physiol.* **590**, 809-825.

Saffen, D. W., Cole, A. J., Worley, P. F., Christy, B. A., Ryder, K. and Baraban, J. M. (1988). Convulsant-induced increase in transcription factor messenger RNAs in rat brain. *Proc. Natl. Acad. Sci. USA* **85**, 7795-7799.

Sanyal, S. (2009). Genomic mapping and expression patterns of C380, OK6 and D42 enhancer trap lines in the larval nervous system of Drosophila. *Gene Expr. Patterns* **9**, 371-380.

Sanyal, S. and Ramaswami, M. (2006). Activity-dependent regulation of transcription during development of synapses. *Int. Rev. Neurobiol.* **75**, 287-305.

Sanyal, S., Sandstrom, D. J., Hoeffer, C. A. and Ramaswami, M. (2002). AP-1 functions upstream of CREB to control synaptic plasticity in Drosophila. *Nature* **416**, 870-874.

Sanyal, S., Narayanan, R., Consoulas, C. and Ramaswami, M. (2003). Evidence for cell autonomous AP1 function in regulation of Drosophila motor-neuron plasticity. *BMC Neurosci.* **4**, 20.

Schmitt, S., Evers, J. F., Duch, C., Scholz, M. and Obermayer, K. (2004). New methods for the computer-assisted 3-D reconstruction of neurons from confocal image stacks. *Neuroimage* **23**, 1283-1298.

Séguéla, P., Wadiche, J., Dineley-Miller, K., Dani, J. A. and Patrick, J. W. (1993). Molecular cloning, functional properties, and distribution of rat brain alpha 7: a nicotinic cation channel highly permeable to calcium. *J. Neurosci.* **13**, 596-604.

Sin, W. C., Haas, K., Ruthazer, E. S. and Cline, H. T. (2002). Dendrite growth increased by visual activity requires NMDA receptor and Rho GTPases. *Nature* **419**, 475-480.

Sweeney, N. T., Li, W. and Gao, F. B. (2002). Genetic manipulation of single neurons in vivo reveals specific roles of flamingo in neuronal morphogenesis. *Dev. Biol.* **247**, 76-88.

Tripodi, M., Evers, J. F., Mauss, A., Bate, M. and Landgraf, M. (2008). Structural homeostasis: compensatory adjustments of dendritic arbor geometry in response to variations of synaptic input. *PLoS Biol.* **6**, e260.

Van Aelst, L. and Cline, H. T. (2004). Rho GTPases and activity-dependent dendrite development. *Curr. Opin. Neurobiol.* **14**, 297-304.

Vonhoff, F. and Duch, C. (2010). Tiling among stereotyped dendritic branches in an identified Drosophila motoneuron. *J. Comp. Neurol.* **518**, 2169-2185.

Vonhoff, F., Williams, A., Ryglewski, S. and Duch, C. (2012). *Drosophila* as a model for MECP2 gain of function in neurons. *PLoS ONE* **7**, e31835

Wang, J., Renger, J. J., Griffith, L. C., Greenspan, R. J. and Wu, C. F. (1994). Concomitant alterations of physiological and developmental plasticity in Drosophila CaM kinase II-inhibited synapses. *Neuron* **13**, 1373-1384.

Wang, Z., Palmer, G. and Griffith, L. C. (1998). Regulation of Drosophila Ca2+/calmodulin-dependent protein kinase II by autophosphorylation analyzed by site-directed mutagenesis. *J. Neurochem.* **71**, 378-387.

Warp, E., Agarwal, G., Wyart, C., Friedmann, D., Oldfield, C. S., Conner, A., Del Bene, F., Arrenberg, A. B., Baier, H. and Isacoff, E. Y. (2012). Emergence of patterned activity in the developing zebrafish spinal cord. *Curr. Biol.* **22**, 93-102.

Watson, M. R., Lagow, R. D., Xu, K., Zhang, B. and Bonini, N. M. (2008). A drosophila model for amyotrophic lateral sclerosis reveals motor neuron damage by human SOD1. *J. Biol. Chem.* **283**, 24972-24981.

West, A. E. and Greenberg, M. E. (2011). Neuronal activity-regulated gene transcription in synapse development and cognitive function. *Cold Spring Harb. Perspect. Biol.* **3**, a005744.

West, A. E., Griffith, E. C. and Greenberg, M. E. (2002). Regulation of transcription factors by neuronal activity. *Nat. Rev. Neurosci.* **3**, 921-931.

Wu, G., Malinow, R. and Cline, H. T. (1996). Maturation of a central glutamatergic synapse. *Science* **274**, 972-976.

Wu, G. Y., Deisseroth, K. and Tsien, R. W. (2001). Spaced stimuli stabilize MAPK pathway activation and its effects on dendritic morphology. *Nat. Neurosci.* **4**, 151-158.

Yao, K. M. and White, K. (1994). Neural specificity of elav expression: defining a Drosophila promoter for directing expression to the nervous system. *J. Neurochem.* **63**, 41-51.

Yeh, E., Gustafson, K. and Boulianne, G. L. (1995). Green fluorescent protein as a vital marker and reporter of gene expression in Drosophila. *Proc. Natl. Acad. Sci. USA* **92**, 7036-7040.

Zhu, H. and Luo, L. (2004). Diverse functions of N-cadherin in dendritic and axonal terminal arborization of olfactory projection neurons. *Neuron* **42**, 63-75.

Zuo, Y., Lin, A., Chang, P. and Gan, W. B. (2005). Development of long-term dendritic spine stability in diverse regions of cerebral cortex. *Neuron* **46**, 181-189.

DEVELOPMENT